NEOPLASIA
www.neoplasia.com
Volume 23 Number xxx Month 2021 pp. 731–742

Original Research

On the origin of germ cell neoplasia in situ: Dedifferentiation of human adult Sertoli cells in cross talk with seminoma cells in vitro ☆

Cornelia Fink [a,*]; Nelli Baal [b]; Jochen Wilhelm [c,i]; Poonam Sarode [d]; Roswitha Weigel [a]; Valérie Schumacher [e]; Daniel Nettersheim [f]; Hubert Schorle [g]; Carmen Schröck [a]; Martin Bergmann [a]; Sabine Kliesch [h]; Monika Kressin [a]; Rajkumar Savai [c,d,i,*]

[a] Department of Veterinary Anatomy, Histology and Embryology, Justus-Liebig-University Giessen, Giessen, Germany
[b] Institute for Clinical Immunology and Transfusion Medicine, Universities of Giessen and Marburg, Giessen, Germany
[c] Department of Internal Medicine, Member of the German Center for Lung Research (DZL), Germany
[d] Department of Lung Development and Remodelling, Max Planck Institute for Heart and Lung Research, Member of the DZL, Member of CPI, Bad Nauheim, Germany
[e] Department of Urology and Medicine, Boston Children's Hospital, Department of Surgery and Pediatrics, Harvard Medical School, Boston, MA, USA
[f] Department of Urology, Urological Research Lab, Translational UroOncology, University Hospital Düsseldorf, Düsseldorf, Germany
[g] University Hospital Bonn, Department of Developmental Pathology, Institute of Pathology, Bonn, Germany
[h] University of Münster, Centre of Andrology and Reproductive Medicine, Münster, Germany
[i] Institute for Lung Health (ILH), Justus-Liebig-University, Giessen, Germany

Abstract

Germ cell neoplasia in situ (GCNIS) is the noninvasive precursor of testicular germ cell tumors type II, the most common cancer in young men, which originates from embryonic germ cells blocked in their maturation. GCNIS is associated with impaired Sertoli cells (SCs) that express fetal keratin 18 (KRT18) and the pluripotency factor SRY-Box transcription factor 2 (SOX2). According to the current theory concerning the origin of GCNIS, these SCs are prepubertal cells arrested in their maturation due to (epi)genetic anomalies and/or environmental antiandrogens. Thus, they are unable to support the development of germ cells, which leads to their maturational block and further progresses into GCNIS. Alternatively, these SCs are hypothesized to be adult cells dedifferentiating secondarily under the influence of GCNIS. To examine whether tumor cells can dedifferentiate SCs, we established a coculture model of adult human SCs (FS1) and a seminoma cell line similar to GCNIS (TCam-2). After 2 wk of coculture, FS1 cells showed progressive expression of KRT18 and SOX2, mimicking the in vivo changes. TCam-2 cells showed SOX2 expression and upregulation of further pluripotency- and reprogramming-associated genes, suggesting a seminoma to embryonal carcinoma transition. Thus, our FS1/TCam-2 coculture model is a valuable tool for investigating interactions between SCs and seminoma cells. Our immunohistochemical and ultrastructural studies of human testicular biopsies with varying degrees of GCNIS compared to biopsies from fetuses, patients with androgen insensitivity syndrome, and patients showing normal spermatogenesis further suggest that GCNIS-associated SCs represent adult cells undergoing progressive dedifferentiation.

Neoplasia (2021) 23, 731–742

Keywords: Germ cell neoplasia in situ, Sertoli cell dedifferentiation, TCam-2 seminoma cell line, Coculture model, Microenvironment

* Corresponding authors.
E-mail addresses: Cornelia.Fink@vetmed.uni-giessen.de (C. Fink), Rajkumar.Savai@mpi-bn.mpg.de (R. Savai).
☆ Conflicts of interest: The authors declare that they have no known competing financial interests or personal relationships that could have appeared to influence the work reported in this paper.
Received 20 January 2021; received in revised form 19 May 2021; accepted 19 May 2021

https://doi.org/10.1016/j.neo.2021.05.008

Introduction

Germ cell neoplasia in situ (GCNIS) is the noninvasive precursor of testicular germ cell tumors type II (TGCT), which accounts for up to 60% of all malignancies diagnosed in Caucasian men aged 20 to 40-y old [1,2]. The TGCT incidence rate has increased by 70% over the last 20 y [3,4]. Despite extensive research, TGCT etiology remains unclear. Defined risk factors for TGCT are cryptorchidism [5], infertility [6], and familial predisposition [7]. In addition, genome-wide association studies have indicated an association between a number of single-nucleotide polymorphisms and TGCT [8,9]. Environmental influences, such as exposure to androgen disrupters, lifestyle factors, and perinatal characteristics have no clear associations with TGCT [10,11]. It is likely that the combined action of (epi)genetic and (micro)environmental factors leads to TGCT [12].

The current model of TGCT pathogenesis (Fig. 1A) states that GCNIS originates from embryonic germ cells—either primordial germ cells (PGC) or gonocytes—blocked in their maturation [13]. The causes of the developmental arrest of PGC/gonocytes are unknown. After puberty, GCNIS eventually progress into seminoma, which is similar to GCNIS and PGC with respect to gene expression and histology [13,14] or reprogram the pluripotency into embryonal carcinoma (EC) [13]. GCNIS, seminomas, and EC express the pluripotency markers OCT3/4 and NANOG, but pluripotency transcription factor SOX2 is only expressed by EC [15].

Tumorigenesis is strongly influenced by nonmalignant cells that comprise the tumor microenvironment [16]. Interestingly, GCNIS cells occupy the spermatogonial niche of the adult testis together with Sertoli cells (SCs) that are impaired in their differentiation [17,18].

SCs must differentiate from an immature fetal phenotype to an adult phenotype to support spermatogenesis [19]. This terminal differentiation during puberty is defined by changes in their morphology [20], the conversion to a nonproliferative state, the formation of the blood-testis barrier (BTB), and changes in their protein expression profile [19]. For example, SCs in fetal testes express keratin 18 (KRT18) and vimentin (VIM), whereas SCs in adult testes express VIM only [21,22]. Most of the fetal marker KRT18 is lost at a gestational age of 20 wk, and it is completely absent around birth, signaling the earliest transition of SCs to a mature state [17,23]. The expression of androgen receptor (AR), by contrast, begins in late puberty and is a hallmark of adult SCs [19,24]. SCs in GCNIS-containing tubules of adult testis are positive for AR [25], but they also express KRT18 [17,26] and SOX2 [27]. SOX2 is not expressed in fetal gonads from 15 wk of gestation onward, indicating either aberrant expression of SOX2 in GCIN-associated SCs or persistent expression, assuming that SOX2 is expressed before 15 wk of gestation [27].

According to the current hypothesis, SCs associated with GCNIS are prepubertal cells arrested in their differentiation due to genetic anomalies and/or environmental agents like xeno-estrogens and antitestosterones. The immature SCs fail to stimulate the germ cells and constitute a microenvironment that allows PGC/gonocytes to survive in the postnatal testes. The PGC/gonocytes that fail to differentiate into prespermatogonia may further develop into GCNIS [28–30]. However, there has been an ongoing discussion on whether the impaired SCs are immature cells contributing to the development of GCNIS (Fig. 1A, Theory 1) or adult cells that dedifferentiate under the influence of GCNIS and/or the underlaying pathological process (Fig. 1A, Theory 2). The second theory is supported by evidence that adult SCs are capable of dedifferentiation. For example, KRT18 is re-expressed in monkey testes following heat treatment [31].

Testing these hypotheses is immensely difficult due to the inaccessibility of the fetal testis (where dysgenesis would occur) and the lengthy time period (20–45 y) before outcomes can be observed. Because of the lack of suitable model systems for GCNIS, experimental testing is not yet possible [32,33]. Furthermore, while stroma reprogramming in carcinomas is well described, stromal changes in benign forms of tumors remain poorly characterized [34]. To our knowledge, no studies concerning the possible reciprocal influences of GCNIS/seminoma cells and SCs have been conducted.

For the present study, we established a coculture model with the adult human SC line FS1 [35] and the seminoma cell line TCam-2 [36] to determine whether seminoma cells can dedifferentiate SCs. Furthermore, we conducted immunostaining and ultrastructural studies of SCs in human testicular biopsies with varying degrees of GCNIS and compared our findings with normal spermatogenesis (nsp), fetal testes from 6 wk of gestation onward, and prepubertal seminiferous cords of patients with androgen insensitivity syndrome (AIS).

Materials and methods

Materials and methods for *cell lines and cell culture, human samples, RNA isolation, cDNA synthesis, and reverse transcription-PCR (RT-PCR), immunostaining, cell proliferation assessment of FS1 and TCam-2 cells in monoculture and direct coculture by cell counting method, RNA isolation and microarray analysis, analysis of secretory factors in conditioned media (CM) by proteome profiler human XL cytokine array,* and *histomorphometric analysis of SOX2 and KRT18 expression on serial sections with varying degrees of GCNIS* can be found in the online supplement.

Cell coculture model

For direct coculture, FS1 cells were cultured in 24-well plates. After 24 h, the medium was replaced by 1:1 mixture of medium I [4.5 g/l D-glucose, 40 µM L-glutamine (Sigma), 1% sodium pyruvate (Gibco, by Life Technologies), 20% fetal calf serum (PAA Laboratories GmbH), 1% nonessential amino acids, and 1% penicillin/streptomycin] and medium II [Rosewell Park Memorial Institute 1640 medium (Gibco) and supplemented with 2 µM L-glutamine, 10% fetal calf serum, and 1% penicillin/streptomycin], and TCam-2 cells were added in 2 different proportions: 7500 FS1 + 7500 TCam-2 cells/well and 5000 FS1 + 10,000 TCam-2 cells/well, followed by 2 or 3 wk of coculture at 37°C and 5% CO_2 in 2-to-3-d rotations.

For indirect coculture, we used 6 well ThinCert (Greiner Bio-One) cell culture inserts with translucent membranes (0.4 μm). We seeded 50,000 FS1 and TCam-2 cells in the apical chamber on the upper side and the underside of the membrane, respectively. In further experimental settings, TCam-2 cells were seeded in the insert and FS1 cells in the 6 well plate. The cells were cocultured for 3 wk in a 1:1 mixture of medium I and II at 37°C and 5% CO_2 in a 2-to-3-d rotation.

For control, FS1 cells were cultured in direct and indirect coculture with equine-bone-marrow-derived mesenchymal stromal cells (eBM-MSC) provided by Prof. Dr. C. Staszyk, Department of Veterinary Anatomy, Histology, and Embryology, Justus-Liebig-University, Giessen, Germany. For further controls, FS1 and TCam-2 monocultures of 15,000 cells/well were used. For each condition, 4 biological and 10 technical replicates were generated.

Fluorescence-activated cell sorting (FACS)

There were no data in the literature regarding surface antigens for FS1 and TCam-2 cells. Thus, we selected several markers for phenotyping from the Human Cell Surface Marker Screening (PE) Kit (Biolegend) based on the mRNA expression of each cell line in the microarray data, with the criterion of "genes expressed by FS1 cells but not by TCam-2 cells". Samples were stained according to the manufacturer's instructions with fluorochrome-labeled human monoclonal antibodies or appropriate isotype controls for 30 min at 4°C and washed with HBSS (300 g for 5 min at 4°C) before analysis.

For sorting, FS1 and TCam-2 cells were cocultivated in 75-cm^2 flasks. Around day 12 of coculture, we harvested and sorted the cells by FACS

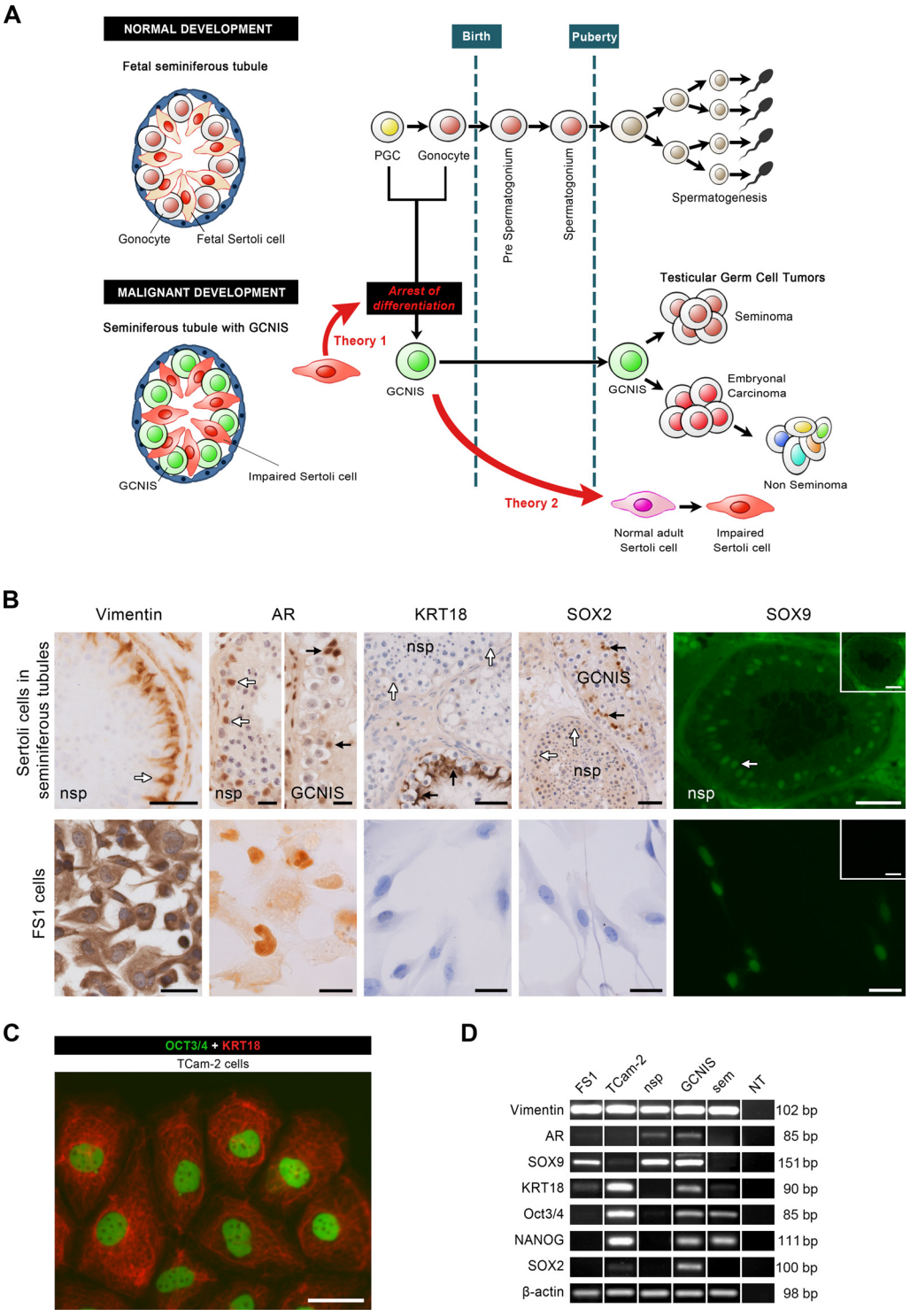

Fig. 1. Model of testicular germ cell tumor type II (TGCT) development and comparison of FS1 and TCam-2 cells with sections of testicular biopsies. (A) Model of TGCT development (modified from Rajpert-De Meyts, 2006 [29]). Differentiation arrest in PGC or gonocytes during prenatal development leads to GCNIS in seminiferous tubules. From puberty, GCNIS cells may begin to transform into seminoma, nonseminomas, or both. GCNIS is associated with impaired SCs. The current hypothesis suggests that the impaired SCs are prepubertal cells arrested in their differentiation. They are unable to support normal spermatogonial development, leading to the differentiation arrest of germ cells (Theory 1). Alternatively, it is hypothesized that these SCs are adult cells that are dedifferentiating under the influence of GCNIS and/or the underlying pathological process (Theory 2). (B) Immunoreactivity of FS1 cells compared with SCs in seminiferous tubules. SCs in seminiferous tubules containing nsp (white arrows) as well as FS1 cells show cytoplasmic staining for VIM and nuclear staining for AR and SOX9. Both are negative for KRT18 and SOX2. Impaired SCs in tubules with GCNIS (black arrows) are also positive for AR, but they additionally express KRT18 and SOX2. Insets: Negative controls. Scale bars = 50 µm. Scale bars for AR in nsp, GCNIS, and FS1 = 20 µm. (C) TCam-2 cells show nuclear staining for OCT3/4 and cytoplasmic staining for KRT18 filaments. Scale bar = 50 µm. (D) RT-PCR reaction products from FS1, TCam-2, nsp, GCNIS, and seminoma (sem). ß-actin, loading control; NT, no template.

for the surface antigen CD73 (7355, Biolegend). From the CD73-negative cells, we collected TRA-1-60-R-positive (5389, Biolegend) and TRA-1-60-R-negative cell fractions. The cells were sorted into 1.5-mL tubes with 500 μL RNase-free PBS. FCM analysis and sorting were conducted on a Canto II cell sorter (BD) and data were analyzed using the FACSdiva version 6.1.2 software (BD). Nonspecific staining of the selected antibodies was determined using the corresponding isotype controls.

After sorting, cell pellets were snap-frozen with liquid N2 and then stored at −80°C. The remaining sorted CD73-positive cells were resuspended in medium I, and the CD73-negative cells were resuspended in medium II and replated separately in cell culture flasks.

Results

Human adult SC line FS1 resembles adult SCs, and TCam-2 cell line resembles seminoma

This study used FS1 cells, which are similar to adult SCs in testicular biopsies, as they are spindle-shaped with long cytoplasmic extensions and contain ovoid or irregular-shaped nuclei with typical deep indentations and prominent nucleoli. As the FS1 cells are reticulated they grew to form a network. Adult SCs in tubules with nsp (Fig. 2B, white arrows) were positive for SC markers VIM and SOX9, and adult SC marker AR. They were negative for the fetal SC marker KRT18 (Fig. 2B, white arrows). Adult SCs were also negative for SOX2 (Fig. 2B, white arrows) aside from a few scattered cells (Supplementary Fig. 1A, arrow). Like adult SCs, FS1 cells expressed VIM, SOX9, and AR (Fig. 2B). Similarly, FS1 cells were negative for KRT18 (Fig. 2B) and SOX2 (Fig. 2B). SCs in GCNIS tubules also expressed VIM (not shown), SOX9 (Fig. 4), and AR (Fig. 2B, black arrows). However, in contrast to SCs in nsp, they were positive for KRT18 and SOX2 (Fig. 2B, black arrows and Supplementary Fig. 1A). We did not detect SOX2 in fetal testis from 6 wk of gestation onward nor in the immature SCs or gonocytes of patients with AIS (Supplementary Fig. 1A).

Because there are no GCNIS cell lines, we used the seminoma cell line TCam-2, which shows similarities to GCNIS [36,37]. For example, whereas tubules with nsp were negative for OCT3/4, GCNIS, seminoma cells (Supplementary Fig. 1B), and TCam-2 cells (Fig. 1C) showed OCT3/4 nuclear staining. Furthermore, like gonocytes, GCNIS (Supplementary Fig. 1A, arrows), and seminoma cells, TCam-2 cells were negative for SOX2 (Fig. 2D–G, empty arrowhead). TCam-2 cells were flat and polygonal with large irregular-shaped nuclei and many prominent nucleoli. They contained cross-striated KRT18 filaments (Fig. 1C). TCam-2 cells grew to form a monolayer.

After performing RT-PCR (Fig. 1D), we confirmed *VIM* and *SOX9* expression in FS1 cells, which resulted in strong specific bands at 102 bp and 151 bp. *AR* was barely detectable. FS1 did not express *OCT3/4, NANOG*, or *SOX2* but did show a weak band for *KRT18* at 90 bp. TCam-2 showed strong *VIM, KRT18, OCT3/4*, and *NANOG* expression. *SOX9* and *SOX2* mRNA bands were barely detectable. Homogenates of human testicular biopsy specimens with nsp expressed *VIM* and *SOX9* (attributable to the SCs) and *AR* (attributable to SCs and peritubular myoid cells). Homogenates with GCNIS furthermore expressed *KRT18* and *SOX2* (attributable to the impaired SCs) as well as *OCT3/4* and *NANOG* (attributable to GCNIS). Seminoma specimens expressed *VIM, OCT3/4*, and *NANOG* and showed a weak band at 90 bp for *KRT18*.

Bidirectional crosstalk between FS1 and TCam-2 cells induces KRT18 and SOX2 expression

After a 1-wk direct coculture of FS1 and TCam-2, the TCam-2 cells were readily detected expressing OCT3/4 and KRT18 (Fig. 2A, empty arrowhead), while the FS1 cells remained negative for both (Fig. 2A, empty arrows). After 2 wk, the first KRT18-positive FS1 cells appeared, showing the typical spindle shape and longitudinally oriented filaments (Fig. 2B, white arrow). After 3 wk, KRT18-positive FS1 cells increased considerably in number (Fig. 2C, white arrow). Using triple immunofluorescence (IF) against OCT3/4, KRT18, and SOX2 after 2 and 3 wk of coculture, we still found unchanged FS1 cells (Fig. 2D, empty arrow). However, we additionally observed FS1 cells expressing KRT18 (Fig. 2E, white arrow) and coexpressing KRT18 and SOX2 (Fig. 2F, white arrow). These altered FS1 cells were mostly seen in close contact with TCam-2 cells, but we also found altered FS1 cells that were further away from the TCam-2 cells (Fig. 2C, white arrow). FS1 cells in the control groups of monoculture or direct coculture with eBM-MSC did not express KRT18 and/or SOX2 during the same time frame (Supplementary Fig. 2A–D). Interestingly, about 30% of the TCam-2 cells expressed SOX2 after 2 and 3 wk of coculture with FS1 (Fig. 2F and G, white arrowhead).

To investigate distant effects on KRT18 and SOX2 expression, we used 2 different approaches to perform FS1/TCam-2 indirect coculture. In the first, we cocultured FS1 cells on one side of the membrane and TCam-2 cells on the other side. FS1 cells expressing KRT18 were fewer than after direct coculture, whereas a large number of TCam-2 cells showed SOX2 expression (Supplementary Fig. 2E, 2F). In the second approach, when TCam-2 cells were seeded in the insert and FS1 cells on the bottom of the 6 well plate, we detected only single FS1 cells positive for KRT18.

Bidirectional crosstalk between FS1 and TCam-2 cells increases proliferation of FS1 cells and induces embryonal carcinoma-associated genes in TCam-2 cells

To assess the proliferation of FS1 and TCam-2 in coculture, both cell lines were cultured in monoculture and coculture for 2 wk (Fig. 2H). Cocultured FS1 cells showed a 5-fold increase in their cell number compared with monoculture, while cocultured TCam-2 cells showed no significant change in cell number between mono- and coculture (Fig. 2I).

Microarray analysis of 3 wk of monocultures and indirectly cocultured FS1 and TCam-2 cells revealed significant transcriptional alterations after coculture in TCam-2 cells but not in FS1 cells (Supplementary Fig. 3). FS1 cells showed mRNA expression of *KRT18* but not *SOX2* in monoculture and coculture. In TCam-2 cells, *SOX2* expression was very low in monoculture but about 25 times higher after coculture ($P< 0.001$). Interestingly, additional pluripotency- and reprogramming-associated genes were significantly upregulated in TCam-2 during coculture, including *LEFTY1/2, GAL, DPPA5, NODAL, ZIC3, DND1, DPPA3, GDF3, BCAT1, JARID2*, and *DNMT3B* (Fig. 2J).

Crosstalk of FS1 and TCam-2 cells significantly alters their secretory profile

To explore the mechanisms of paracrine regulation, the Human XL Cytokine Array ARY022 including 102 specific antibodies was used. As shown in Supplementary Fig. 4, Cystatin-C, EMMPRIN, IGFBP-2, GDF-15, CD14, and Angiogenin showed significant upregulation in the conditioned medium of the FS1 + TCam-2 coculture compared to monocultures (FS1, TCam-2) and the FS1 + eBM-MSC coculture.

SCs associated with different degrees of GCNIS show sequential expression of SOX2 and KRT18

We performed histomorphometric analysis on testicular sections with varying degrees of GCNIS to assess whether SOX2 and KRT18 expression in SCs associated with GCNIS represent a no-growth stage or a progressive

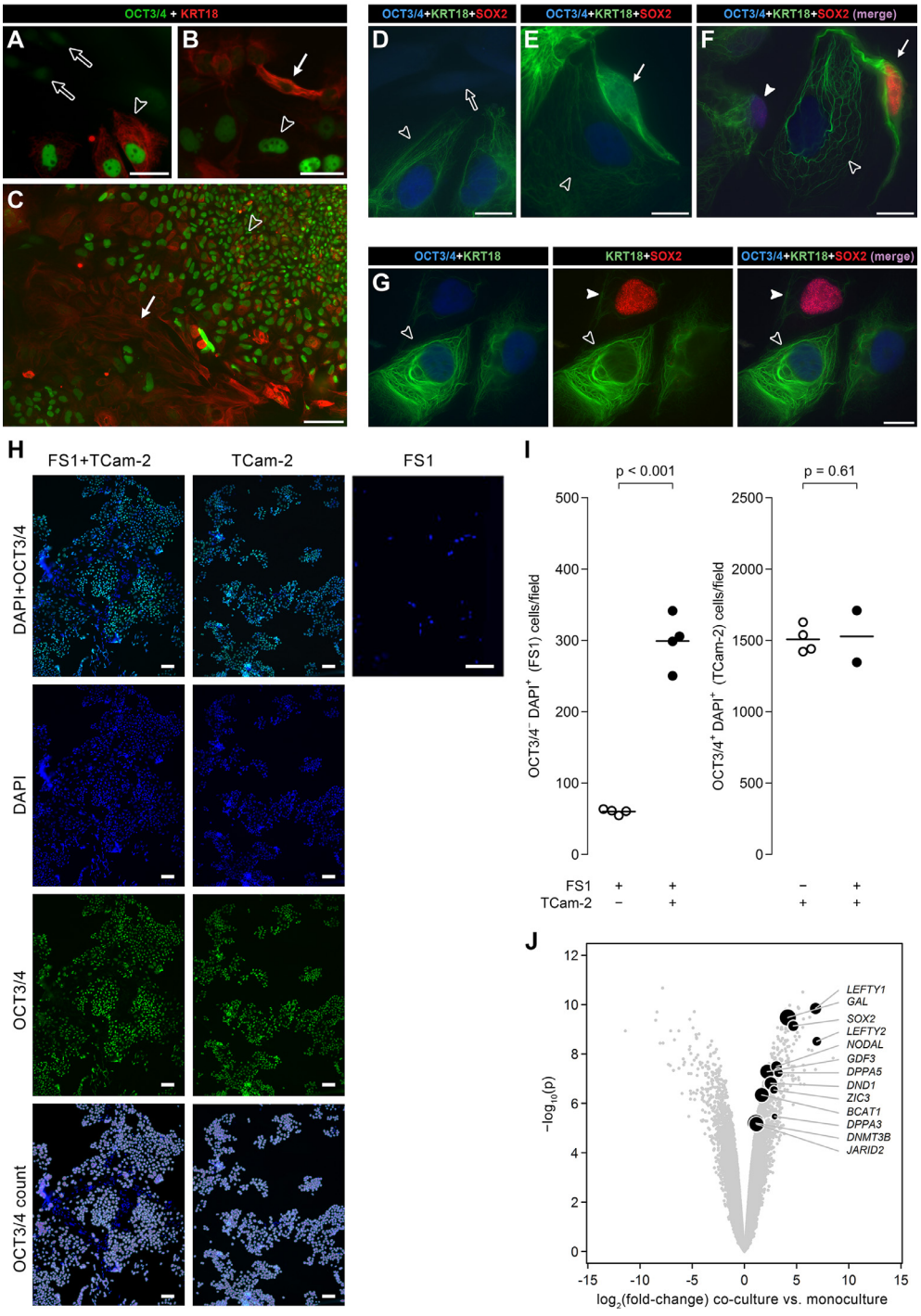

Fig. 2. Bidirectional crosstalk of FS1 and TCam-2 cells induces KRT18 and SOX2 expression and affects cell number and gene expression. (A–C) Double IF for OCT3/4 and KRT18 of FS1 and TCam-2 coculture. (A) After 1 wk, FS1 cells remained negative for OCT3/4 and KRT18 (empty arrows). TCam-2 cells (empty arrowhead) were positive for nuclear OCT3/4 and KRT18 filaments. Scale bar = 50 µm. (B) After 2 wk, the first FS1 cells expressing KRT18 appeared (white arrow). Scale bar = 50 µm. (C) After 3 wk, many KRT18-positive FS1 cells (white arrow) were seen between TCam-2 colonies (empty arrowhead). Scale bar = 100 µm. (D–G) Triple IF for OCT3/4, KRT18, and SOX2. Scale bars = 20 µm. (D) FS1 cells remaining unstained (empty arrow) and TCam-2 cells positive for OCT3/4 and KRT18 and negative for SOX2 (empty arrowhead) after 2 wk of coculture. (E) FS1 cell positive for KRT18 (white arrow) attached to a TCam-2 cell (empty arrowhead) after 3 wk of coculture. (F) FS1 cell coexpressing KRT18 and SOX2 (white arrow) in direct contact with a TCam-2 cell (empty arrowhead) after 3 wk of coculture. The white arrowhead indicates an altered TCam-2 cell expressing nuclear SOX2. (G) An altered TCam-2 cell expressing nuclear SOX2 after 2 wk of coculture (white arrowhead) is shown with different combination of channels. The empty arrowhead indicates an unchanged TCam-2 cell negative for SOX2. (H) Representative images of cell proliferation assessment assay of FS1 and TCam-2 cells after 2 wk of coculture compared with monoculture. Scale bars = 10 µm. (I) Cell proliferation assessment (by cell counting method) of FS1 ($OCT3/4^{-}DAPI^{+}$) and TCam-2 ($OCT3/4^{+}DAPI^{+}$), $n = 4$ or 2, geometric means of 10 measurements per well in monoculture and direct coculture. (J) Volcano plot showing the differential expression profile for TCam-2 cells grown in coculture versus monoculture (log_2[fold-change] of the ratio coculture to monoculture), with some highlighted genes labeled. The sizes of the black points indicate the relative expression levels of the respective genes.

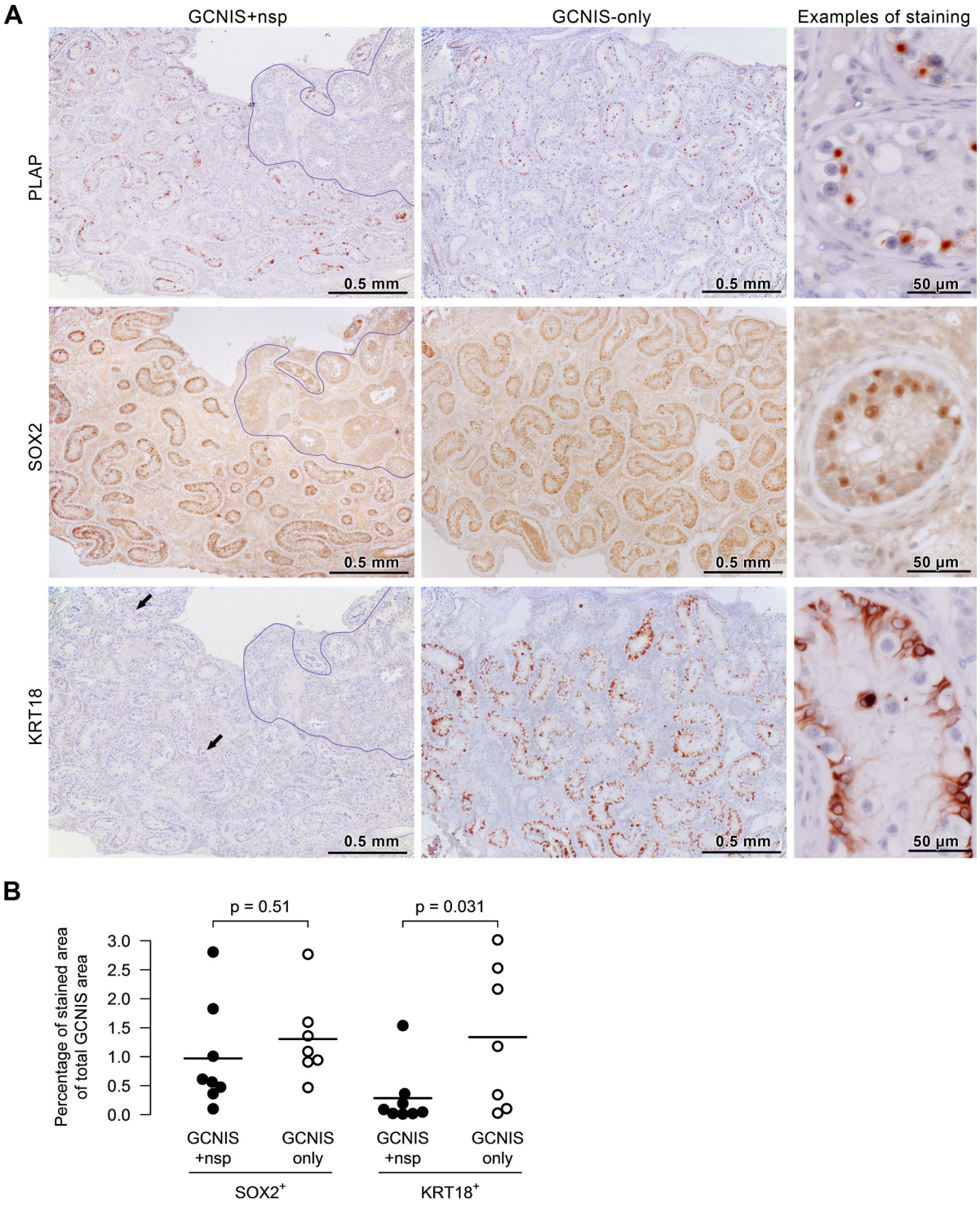

Fig. 3. SCs associated with GCNIS show sequential expression of SOX2 and KRT18. (A) Serial sections of biopsies showing different degrees of GCNIS were stained with PLAP (to confirm GCNIS), SOX2, and KRT18. The area of remaining nsp was delimited by a blue line. In sections of GCNIS + nsp, most of the SCs in GCNIS-containing tubules expressed SOX2, whereas KRT18 expression was scattered (black arrows). In sections showing GCNIS-only, almost all SCs were positive for SOX2 and KRT18. (B) Percentage of stained area of the total GCNIS area ($n = 8$ for GCNIS + nsp, and $n = 7$ for GCNIS-only).

process and whether there is a chronology in their expression. We compared biopsies with 100% GCNIS (GCNIS-only) with biopsies containing 2%, 12%, 45%, 50%, 70%, 75%, 78%, and 93% GCNIS along with remaining nsp (GCNIS + nsp). In GCNIS + nsp and GCNIS-only, SOX2 immunoreactivity was observed in almost all SCs of tubules containing GCNIS (Fig. 3A), with mean values of the stained area around 1% (Fig. 3B). In contrast, KRT18 staining was usually barely detectable in GCNIS + nsp but was widespread in GCNIS-only (mean percentage of stained area = 0.28% and 1.3%, respectively, $P = 0.031$; Fig. 3A and B).

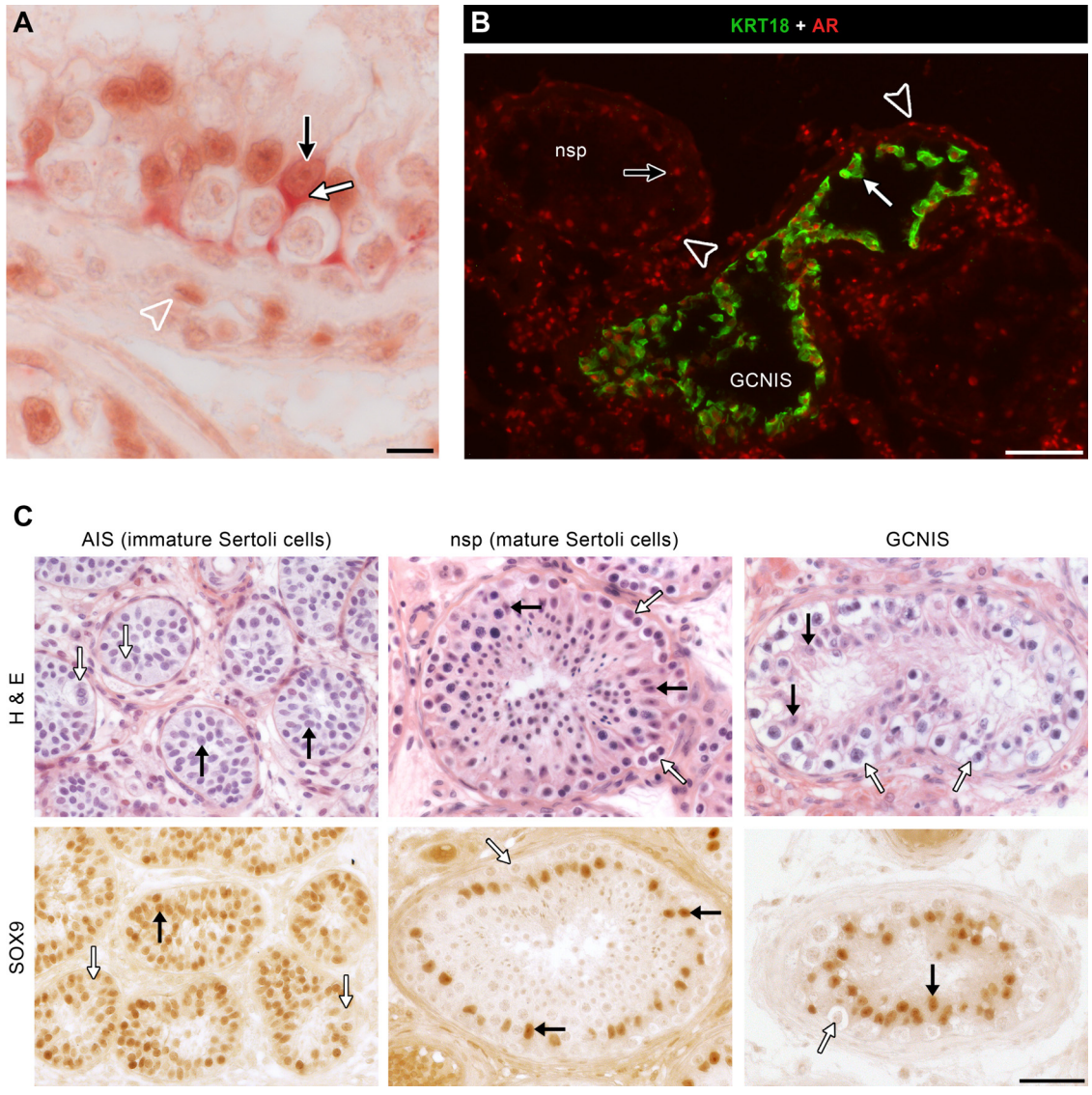

Fig. 4. SCs associated with GCNIS coexpress fetal marker KRT18 and adult marker AR and their morphology resembles the adult SC architecture. (A) Double immunohistochemistry against KRT18 and AR on a paraffin section with GCNIS. SCs showed coexpression of cytoplasmic KRT18 (white arrow) and nuclear AR (black arrow). Peritubular myoid cells also expressed nuclear AR (arrowhead). Scale bar = 10 µm. (B) Double IF on a frozen section containing tubules with GCNIS and nsp. SCs in the tubule with GCNIS showed coexpression of KRT18 and AR (white arrow). SCs in a tubule with nsp only expressed AR (black arrow). Peritubular myoid cells also expressed AR (arrowheads). Scale bar = 100 µm. (C) The seminiferous cords of a 2-y-old patient with AIS contained mainly SCs (black arrows) and scarce gonocytes (white arrows). The SCs show an immature morphology with large, round, and basophilic nuclei containing inconspicuous nucleoli. The seminiferous tubule with nsp depicts different steps of germ cell development from spermatogonia (white arrows) up to maturing spermatids. The SCs show a mature pattern with irregularly outlined, often triangular-shaped nuclei at the basal compartment, which contain prominent nucleoli (H&E, black arrows). The nuclei uniformly "ring" the tubule, which is readily visible by nuclear SOX9 staining (black arrows). The seminiferous tubule containing GCNIS shows atypical germ cells that line the basement membrane (white arrows) and displace SC nuclei to a second row (SOX9, black arrow). SC nuclei show a mature pattern (H&E, black arrows). Scale bar = 50 µm.

SCs associated with GCNIS show coexpression of fetal marker KRT18 and adult marker AR

To investigate whether KRT18 and AR are coexpressed by SCs associated with GCNIS or if they are expressed by different SCs, we performed double immunostaining on paraffin sections (Fig. 4A) and frozen sections (Fig. 4B). We demonstrated the coexpression of cytoplasmic KRT18 (Fig. 4A, white arrow) and nuclear AR (Fig. 4A, black arrow) in the same SC associated with GCNIS for the first time. The frozen sections also showed SCs in GCNIS-containing tubules coexpressing KRT18 and AR (Fig. 4B, white arrow). SCs in tubules with nsp only expressed AR (Fig. 4B, black arrow). Nuclear AR expression was observed in the peritubular myoid cells as well (Fig. 4A, arrowhead and B, arrowheads).

Morphology of SCs associated with GCNIS resembles adult SC architecture

The pubertal maturation of SCs involves morphological changes of the nuclei and cytoplasm. Thus, the cell architecture of immature SCs differs considerably from mature cells. We used light and electron microscopy to

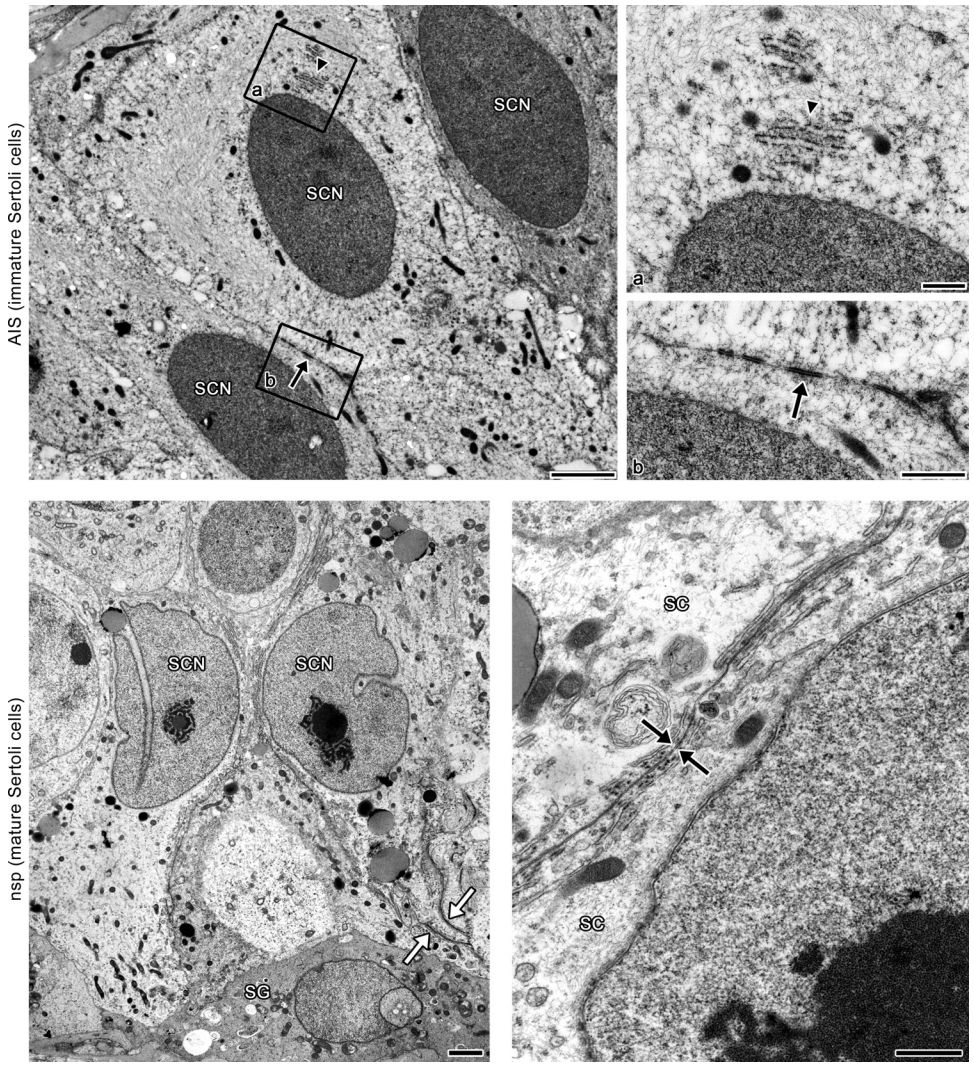

Fig. 5. Ultrastructure of immature SCs in AIS and of adult SCs in nsp. SCs of a 31-y-old patient with AIS are columnar in shape and contain basally located nuclei. The nuclei (SCN) are large, ovoid, and dark and have no prominent nucleoli. The mitochondria are narrow and elongated with a dense matrix. Few lysosomes and lipid droplets are seen. Scale bar = 2.5 µm. Inset a, Single stacks of cisternae of rough ER (arrowhead). Scale bar = 0.5 µm. Inset b, Immature Sertoli cell junctions (arrow). Scale bar = 0.5 µm. Mature SCs at the basal compartment of seminiferous epithelium with nsp show SC nuclei (SCN) with predominant euchromatin, deep indentations, and typical tripartite nucleoli. A Type A spermatogonium (SG) with basal flattening is present on the basal lamina. Lanthanum tracer is present only in the intercellular spaces of the basal compartment (white arrows). Scale bar = 2.5 µm. The black arrows show a typical junctional complex of 2 adjacent SCs (SC), which consists of tight junctions (arrows) with associated bundles of subsurface actin filaments and flat cisternae of ER. Scale bar = 1.0 µm.

analyze the morphology of SCs in GCNIS tubules and to compare it with immature SCs in biopsies from patients with complete AIS [38] and mature SCs in tubules with nsp.

Seminiferous cords of patients with AIS (Fig. 4, AIS) contained abundant SCs and few gonocytes. Little or no lumen was observed. The SCs showed large, rounded, and basophilic nuclei with inconspicuous nucleoli (Fig. 4, AIS-black arrows), displaying a typical immature morphology [20]. The gonocytes were large cells with abundant clear cytoplasm and large, vesicular, euchromatic nuclei containing few strands of heterochromatin (Fig. 4, AIS-white arrows). Mature SCs of tubules with nsp (Fig. 4, nsp-black arrows) contained characteristic eosinophilic, triangular-shaped nuclei with large nucleoli that facilitated their identification within the germinal epithelium. The nuclei were regularly aligned at the base of the cells, forming a ring around the tubule. Many spermatogonia rested on the base of the tubules (Fig. 4, nsp-white arrows). SC nuclei in tubules with GCNIS were eosinophilic and irregular shaped and contained prominent nucleoli and thus corresponded to the adult phenotype (Fig. 4, GCNIS-black arrows). They were displaced to a second row by large atypical germ cells localized on the basement membrane. These GCNIS cells exhibited a clear cytoplasm and irregular-shaped nuclei with prominent nucleoli (Fig. 4, GCNIS-white arrows).

Transmission electron microscopy of SCs of patients with AIS revealed an immature, prepubertal phenotype [38]. They were low columnar cells with dark, ovoid nuclei containing finely dispersed chromatin (Fig. 5, SCN). Their scarce cytoplasm contained sparse organelles, a few lysosomes, and a few lipid droplets. The mitochondria were narrow and elongated with irregularly arranged transverse cristae embedded in a dense matrix. Typical single stacks of cisternae of the rough endoplasmic reticulum (ER) were observed (Fig. 5, Inset a-arrowhead). Immature cell junctions were present between adjacent SCs, which originated from focal points of membrane

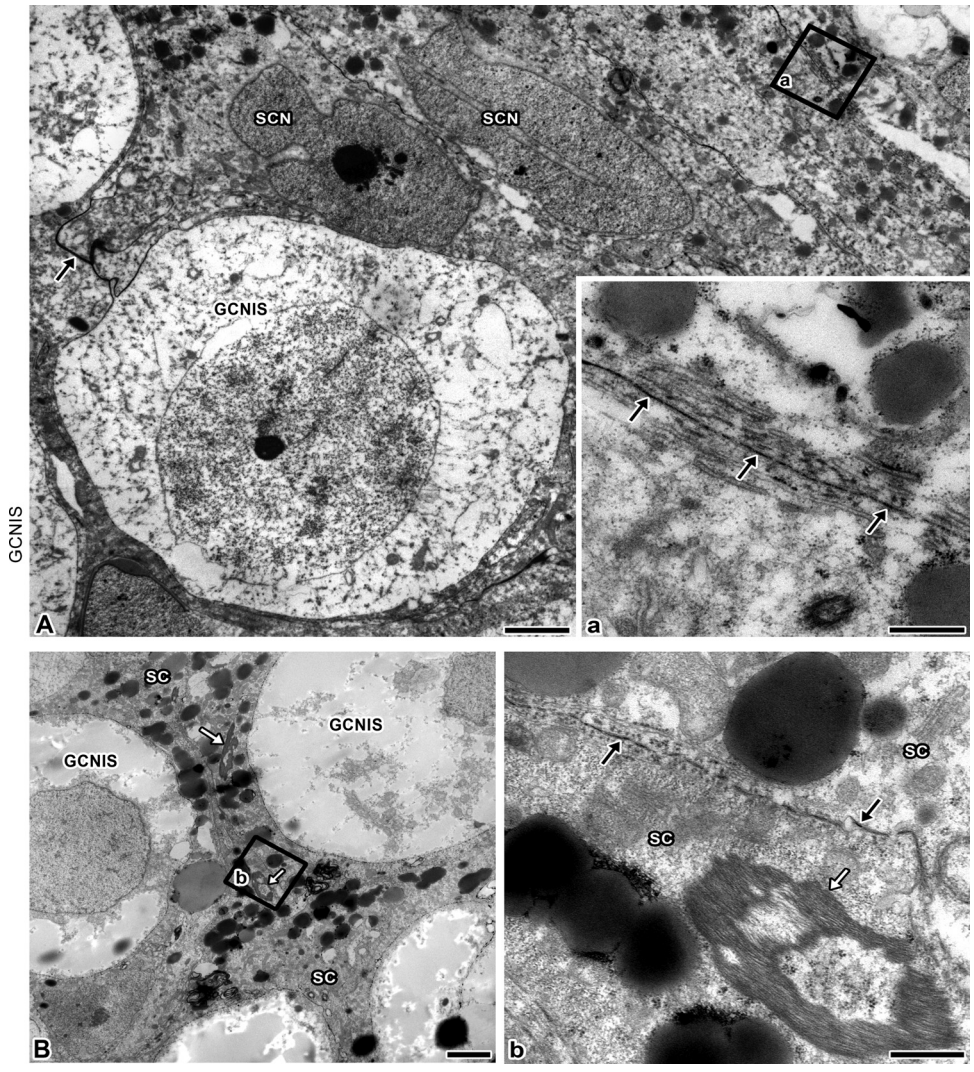

Fig. 6. The ultrastructure of SCs associated with GCNIS resembles adult SCs. (A) SCs show typical mature nuclei (SCN) with irregular and indented outlines and prominent nucleolar complexes. Note the lanthanum tracer passing through the intercellular space (black arrow). Scale bar = 2.5 µm. Inset a, Well-developed inter-Sertoli cell junctional complex showing typical subsurface bundles of actin filaments and associated endoplasmic reticulum. Lanthanum tracer passes through the junctional complex (black arrows), indicating its functional disruption. Scale bar = 0.5 µm. (B) SC (SC) processes separate GCNIS cells from each other and contain Charcot-Böttcher crystalloids (white arrows) and many lipid droplets. Scale bar = 2.5 µm. Inset b, Charcot-Böttcher crystalloid depicting longitudinal fibrillary arrangement and light cores (white arrow). Note the typical inter-SC junctional complex with lanthanum tracer passing through the junctional leaflets (black arrows). Scale bar = 0.5 µm.

approximations (Fig. 5, Inset b-arrow). Mature SCs of tubules with nsp showed irregular-shaped nuclei, usually with one or more deep infoldings (Fig. 5, SCN). Euchromatin was predominant, and heterochromatin was limited to the so-called paranucleolar bodies, which were associated with the nucleolus and thus constitute the tripartite nucleolar complex. Cellular elongation and the elaborate extension of cytoplasmic processes enabled the SCs to establish direct contact with the multiple germ cell layers extending from the base to the lumen. Long, slender mitochondria with a dense matrix and regular-shaped christae, cisternae of smooth ER, and Golgi apparatus were abundant. The cytoplasm also showed numerous secondary lysosomes, lipid vacuoles with indigestible residues, and small, dense granules. Well-developed junctional complexes between adjacent SCs were identified by typical subsurface bundles of actin filaments and associated ER (Fig. 5, black arrows). The actin filaments sandwiched between ER cisternae and the cell membrane formed circumferentially oriented bundles that showed dense amorphous material in cross-sections. These junctional specializations near the base of the epithelium constituted the BTB. The electron-opaque tracer lanthanum nitrate penetrated the intercellular spaces of adjacent SCs and spermatogonia in the basal compartment (Fig. 5, white arrows) and was consistently blocked at the BTB and thus excluded from the adluminal compartment.

SCs in GCNIS tubules displayed morphological features similar to mature SCs. They extended from the basement membrane to the tubular lumen and encircled the GCNIS cells with their cytoplasmic processes. The irregularly formed nuclei showed deep infoldings and prominent nucleoli (Fig. 6, SCN). The cytoplasm contained large accumulations of lipid-like inclusions and residual bodies. The inter-SC junctional complexes were well developed and showed the typical bundles of actin filaments and associated ER cisternae. However, in contrast with nsp, lanthanum tracer passed through the tight junction leaflets, indicating the functional disruption of the BTB (Fig. 6, black arrows). We also found Charcot-Böttcher crystalloids in SCs associated with GCNIS (Fig. 6, white arrows). They were elongated spindle-shaped

structures comprised of longitudinally oriented filaments and displayed light cores occupied by cytoplasmic matrix and a granular material (Fig. 6, Inset b, white arrow). We observed one crystalloid per SC and, furthermore, annulate lamellae (not shown).

Newly identified surface markers for FS1 cells: CD59, CD73, and CD326

We identified 3 novel surface markers for FS1 cells: CD59, CD73, and CD326. FS1 cells were negative for CD24, CD140a, CD324, LTbR, TRA-60-R, and TRA-1-81 (Supplementary Fig. 5A). Most of the TCam-2 cells were positive for CD59 and CD326. Approximately 50% of the TCam-2 cells were positive for CD324 and TRA-1-60-R. TCam-2 cells were negative for CD24, CD73, CD140a, and LTbR (Supplementary Fig. 5B). Therefore, we chose CD73 to identify FS1 cells and to rule out TCam-2 cells for sorting after direct coculture. From the CD73-negative cells (TCam-2), we collected TRA-1-60-R positive and TRA-1-60-R negative cell fractions (Supplementary Fig. 5C). From the replated cells, the CD73-positive population exhibited a spindle-like morphology typical for FS1 cells. Both CD73-negative cell fractions showed the flat polygonal morphology typical of TCam-2.

Discussion

TGCT are considered to be a part of the testicular dysgenesis syndrome [28], a group of disorders believed to arise from the disturbed development of the somatic cells in the gonads, which is likely caused by a disruption in the hormonal microenvironment of the fetus. GCNIS is associated with impaired SCs that have been theorized as being immature cells arrested in their differentiation. Disrupted SC function may fail to elicit gonocyte differentiation, leading to GCNIS development [19,28–30]. Nevertheless, the degree of testicular dysgenesis is inversely related to the incidence of GCNIS [39].

Our aim was to discern whether impaired SCs are prepubertal cells contributing to GCNIS or adult cells secondarily dedifferentiating due to GCNIS. We established a coculture model with the adult human SC line FS1 and the seminoma cell line TCam-2. FS1 cells were dedifferentiated by direct coculturing with TCam-2 cells. They expressed KRT18 and SOX2, mimicking typical in vivo protein alterations. These changes were detected from day 14 and increased progressively. In contrast to KRT18 protein, *KRT18* mRNA was detected in FS1 cells in coculture with TCam-2 and in monoculture. These data support post-translational regulation of KRT18 [40]. Remarkably, we also observed TCam-2 cells expressing SOX2 after coculture with FS1, a transcription factor generally restricted to carcinomas. Nettersheim et al demonstrated that TCam-2 cells upregulated SOX2 after xenografting into the murine flank, where they underwent a transition from seminoma to EC [41]. In line with that study, TCam-2 cells showed upregulation of additional EC-, pluripotency-, and reprogramming-associated genes. Thus, TCam-2 cells upon coculture with FS1 seem to reprogram into EC.

In men, only immature SCs are proliferative. However, Tarulli et al [42] identified a few SCs with PCNA reactivity in men after gonadotropin suppression as well as adjacent to seminoma, while PCNA was absent in SCs in tubules with GCNIS. The authors suggested that adult human SCs are not terminally differentiated and have the capacity to dedifferentiate. In our study, the cell number of FS1 after 2 wk in coculture with TCam-2 was 5 times higher than in monoculture, indicating a loss of differentiation as well.

KRT18 and SOX2 expression in FS1 cells was considerably less after indirect coculture with TCam-2 cells than after direct coculture. Therefore, it is advantageous to perform direct coculture and to sort the FS1 and TCam-2 cells afterward via FACS for further analysis. We identified 3 novel surface markers for FS1 (CD59, CD73, and CD326), of which CD73 was valuable for ruling out TCam-2 cells.

In biopsies containing GCNIS together with remaining nsp, most SCs in tubules with GCNIS expressed SOX2, whereas KRT18 staining was usually scarce. By contrast, in biopsies showing only GCNIS, SOX2 and KRT18 expression was abundant. Assuming that GCNIS-only is a more advanced stage than GCNIS + nsp, SCs associated with dysplastic germ cells would first express SOX2. KRT18 expression would occur later and indicate a progressive process. These data are in line with Kliesch et al [26], who reported that KRT18 expression in SCs was directly correlated with increasing numbers of GCNIS cells. The progressive impairment of SCs in correlation with the degree of GCNIS was also demonstrated by the gradual loss of connexin 43 [43]. Similarly, Nistal et al described inhibin bodies as new markers for immature SCs, having observed them in SCs associated with GCNIS-only but not in GCNIS with remaining spermatogenesis [44]. The progressive impairment of SCs provides evidence for the theory that SCs dedifferentiate due to the influence of GCNIS or the underlying pathological process.

SCs in tubules with GCNIS express both the fetal marker KRT18 and the adult marker AR. However, thus far, it has not been determined whether both markers are expressed by the same SC or whether they are expressed by different SCs in the same tubule. The latter would indicate the coexistence of mature and immature SCs. We demonstrated the coexpression of KRT18 and AR by the same SCs in tubules with GCNIS. The fact that these SCs coexpress KRT18 and AR but not the transitional maturation markers M2A and AMH [45], which losses are bracket temporally by the loss of KRT18 [46] and the expression of AR [24], suggests a partial phenotypic reversion from their previous adult state.

The abundant and apparently early expression of SOX2 in SCs associated to GCNIS is remarkable. SOX2 was not expressed in adult SCs in nsp, except in a few scattered cells, which is in line with the findings of de Jong et al [27]. We did not find SOX2 expression in fetal gonads from 6 wk of gestation onward nor in immature SCs of patients with AIS. Therefore, SOX2 expression in SCs associated to GCNIS seems to be rather an aberrant expression than a persistent expression or re-expression.

The maturation status of SCs is associated with typical morphological features [20]. Skakkebaek et al [47] described apparently normal SCs when they first reported GNCIS in 1972. Nielsen et al [48], in studying the fine structure of GCNIS, indicated that the SCs showed no deviation from the normal ultrastructure nor did they have the appearance of immature SCs. Despite these findings, many authors refer to SCs associated with GCNIS as immature or dysgenetic. Due to these contradictory reports, we studied the morphology of SCs associated with GCNIS to further detail and compared it to immature and mature SCs. We found that the morphology of SCs associated with GCNIS resembles that of adult SCs. We also observed Charcot-Böttcher crystalloids and annulated lamellae, which are further distinguishing features of adult SCs [49,50], 50]. Our interpretation was supported by the ultrastructural appearance of well-developed SC junctional complexes, one of the most sensitive indicators of SC maturation [38]. The only alteration observed was the functional disruption of the BTB that we already reported and attributed to the progressive dislocation of ZO-1, ZO-2 [51], and claudin-11 [52] from the BTB into the cytoplasm. Thus, no morphological support was found for the assumption that the development of the abnormal germ cells results from abnormal function of immature SCs.

Our finding that GCNIS-associated SCs resemble adult cells is in line with the evidence that GCNIS is found in well-differentiated testicular tissue [53]. In contrast, the GCNIS counterpart gonadoblastoma is a neoplastic precursor lesion found in areas of undifferentiated gonadal tissue or immature testis differentiation [15,33]. GCNIS and gonadoblastoma may occur in different areas of the same dysgenetic gonad depending on the level of testicularization [54]. This may explain why the incidence of GCNIS is inversely related to the degree of testicular dysgenesis.

Deficient SOX9 expression in gonadoblastoma supports the current model of pathogenesis, where immature germ cells—in the absence of well-formed SCs—retain a fetal phenotype and susceptibility to malignant transformations [55]. We postulate that, in contrast to gonadoblastoma, the maturational arrest of gonocytes in fetal testes that leads to GCNIS is explained by a primary anomaly of the gonocytes rather than by a failure of immature SCs to support spermatogonial development. We further hypothesize that the SCs in tubules with GCNIS undergo secondary dedifferentiation postpubertally due to GCNIS and/or the underlying pathological process. The dedifferentiating SCs progressively lose the functions necessary to maintain spermatogenesis, including the BTB. This progressive derangement probably facilitates the proliferation and neoplastic progression of GCNIS cells from puberty onward.

Our coculture model suggests that even seminoma cells can alter their environment and thereby induce dedifferentiation in adult SCs, which mimics the findings in our ex vivo studies. Based on our data, we conclude that SCs associated with GCNIS are adult cells that are secondarily dedifferentiating rather than immature cells contributing to the development of GCNIS. TCam-2 cells in coculture with FS1 cells showed SOX2 expression and upregulation of further pluripotency- and reprogramming-associated genes, suggesting a seminoma-to-EC transition. Our FS1/Tcam-2 coculture model is thus a valuable tool for investigating interactions between SCs and tumor cells.

Authors' contributions

Cornelia Fink: Conceptualization, Methodology, Validation, Investigation, Data Curation, Writing – Original Draft Preparation, Writing – Review & Editing, Visualization, Project Administration, Funding Acquisition, Supervision. Nelli Baal: Investigation. Jochen Wilhelm: Formal Analysis, Visualization. Poonam Sarode: Investigation, Writing – Review & Editing. Roswitha Weigel: Investigation. Valerie Schumacher: Resources. Daniel Nettersheim: Resources. Hubert Schorle: Resources. Carmen Schroeck: Investigation. Martin Bergmann: Resources. Sabine Kliesch: Resources. Monika Kressin: Resources. Rajkumar Savai: Methodology, Validation, Investigation, Writing – Review & Editing, Visualization, Project Administration, Supervision.

Funding

This research was funded by the Deutsche Forschungsgemeinschaft (DFG, German Research Foundation), grant number FI 1729/1-1, individual grant Dr. Cornelia Fink.

Acknowledgments

We acknowledge gratefully the excellent technical assistance of Jutta Dern-Wieloch, A. Hild, Alexandra Hax, and Yanina Knepper.

Supplementary materials

Supplementary material associated with this article can be found, in the online version, at doi:10.1016/j.neo.2021.05.008.

References

[1] Adami HO, Bergström R, Möhner M, Zatoński W, Storm H, Ekbom A, Tretli S, Teppo L, Ziegler H, Rahu M, et al. Testicular cancer in nine northern European countries. *Int J Cancer* 1994;**59**:33–8. doi:10.1002/ijc.2910590108.

[2] Shah MN, Devesa SS, Zhu K, McGlynn KA. Trends in testicular germ cell tumours by ethnic group in the United States. *Int J Androl* 2007;**30**:206–13. doi:10.1111/j.1365-2605.2007.00795.x.

[3] Park JS, Kim J, Elghiaty A, Ham WS. Recent global trends in testicular cancer incidence and mortality. *Medicine (Baltimore)* 2018;**97**:e12390. doi:10.1097/MD.0000000000012390.

[4] Brenner DR, Heer E, Ruan Y, Peters CE. The rising incidence of testicular cancer among young men in Canada, data from 1971-2015. *Cancer Epidemiol* 2019;**58**:175–7. doi:10.1016/j.canep.2018.12.011.

[5] Lip SZ, Murchison LE, Cullis PS, Govan L, Carachi R. A meta–analysis of the risk of boys with isolated cryptorchidism developing testicular cancer in later life. *ArchDis Child* 2013;**98**:20–6.

[6] Jorgensen N, Vierula M, Jacobsen R, Pukkala E, Perheentupa A, Virtanen HE, Skakkebaek NE, Toppari J. Recent adverse trends in semen quality and testis cancer incidence among Finnish men. *Int J Androl* 2011;**34**:e37–48.

[7] Mai PL, Friedlander M, Tucker K, Phillips KA, Hogg D, Jewett MA, Lohynska R, Daugaard G, Richard S, Bonaïti-Pellié C, et al. The International Testicular Cancer Linkage Consortium: a clinicopathologic descriptive analysis of 461 familial malignant testicular germ cell tumor kindred. *Urol Oncol* 2010;**28**:492–9.

[8] Chung CC, Kanetsky PA, Wang Z, Hildebrandt MA, Koster R, Skotheim RI, Kratz CP, Turnbull C, Cortessis VK, Bakken AC, et al. Meta–analysis identifies four new loci associated with testicular germ cell tumor. *Nat Genet* 2013;**45**:680–5.

[9] LeBron C, Pal P, Brait M, Dasgupta S, Guerrero–Preston R, Looijenga LH, Kowalski J, Netto G, Hoque MO. Genome–wide analysis of genetic alterations in testicular primary seminoma using high resolution single nucleotide polymorphism arrays. *Genomics* 2011;**97**:341–9.

[10] Béranger R, Le Cornet C, Schuz J, Fervers B. Occupational and environmental exposures associated with testicular germ cell tumours: systematic review of prenatal and life–long exposures. *PLoS One* 2013;**8**:e77130.

[11] Cook MB, Akre O, Forman D, Madigan MP, Richiardi L, McGlynn KA. A systematic review and meta–analysis of perinatal variables in relation to the risk of testicular cancer – experiences of the mother. *Int J Epidemiol* 2009;**38**:1532–42.

[12] Looijenga LH, Van Agthoven T, Biermann K. Development of malignant germ cells – The genvironmental hypothesis. *Int J Dev Biol* 2013;**57**:241–53.

[13] Almstrup K, Hoei-Hansen CE, Nielsen JE, Wirkner U, Ansorge W, Skakkebaek NE, Rajpert-De Meyts E, Leffers H. Genome-wide gene expression profiling of testicular carcinoma in situ progression into overt tumours. *Br J Cancer* 2005;**92**:1934–41. doi:10.1038/sj.bjc.6602560.

[14] Looijenga LHJ, Kao CS, Idrees MT. Predicting Gonadal Germ Cell Cancer in People with Disorders of Sex Development; Insights from Developmental Biology. *Int J Mol Sci* 2019;**20**:5017–39. doi:10.3390/ijms20205017.

[15] Looijenga LH. Human testicular (non)seminomatous germ cell tumours: the clinical implications of recent pathobiological insights. *J Pathol* 2009;**218**:146–62. doi:10.1002/path.2522.

[16] Mueller MM, Fusenig NE. Friends or foes - bipolar effects of the tumour stroma in cancer. *Nat Rev Cancer* 2004;**4**:839–49.

[17] Rogatsch H, Jezek D, Hittmair A, Mikuz G, Feichtinger H. Expression of vimentin, cytokeratin, and desmin in Sertoli cells of human fetal, cryptorchid, and tumour-adjacent testicular tissue. *Virchows Arch* 1996;**427**:497–502. doi:10.1007/BF00199510.

[18] Nistal M, Gonzalez-Peramato P, Regadera J, Serrano A, Tarin V, De Miguel MP. Primary testicular lesions are associated with testicular germ cell tumors of adult men. *Am J Surg Pathol* 2006;**30**:1260–8. doi:10.1097/01.pas.0000213361.10756.08.

[19] Sharpe RM, McKinnel C, Kivlin C, Fisher JS. Proliferation and functional maturation of Sertoli cells, and their relevance to disorders of testis function in adulthood. *Reproduction* 2003;**125**:769–84. doi:10.1530/rep.0.1250769.

[20] Nistal M, De Mora JC, Paniagua R. Classification of several types of maturational arrest of spermatogonia according to Sertoli cell morphology: an approach to aetiology. *Int J Androl* 1998;**21**:317–26. doi:10.1046/j.1365-2605.1998.00122.x.

[21] Franke WW, Grund C;, Schmid E. Intermediate-sized filaments present in Sertoli cells are of the vimentin type. *Eur J Cell Biol* 1979;**19**(3):269–75.

[22] Bergmann M, Kliesch S. The distribution pattern of cytokeratin and vimentin immunoreactivity in testicular biopsies of infertile men. *Anat Embryol* 1994;**190**:515–20. doi:10.1007/BF00190101.

[23] Franke FE, Pauls K, Rey R, Marks A, Bergmann M, Steger K. Differentiation markers of Sertoli cells and germ cells in fetal and early postnatal human testis. *Anat Embryol* 2004;**209**:169–77. doi:10.1007/s00429-004-0434-x.

[24] Suárez-Quian CA, Martinez-Garcia F, Nistal M, Regadera J. Androgen receptor distribution in adult human testis. *J Clin Endocrinol Metab* 1999;**84**:350–8. doi:10.1210/jcem.84.1.5410.

[25] Rajpert-De Meyts E, Skakkebaek NE. Immunohistochemical identification of androgen receptors in germ cell neoplasia. *J Endocrinol* 1992;**135**:R1–4. doi:10.1677/joe.0.135r001.

[26] Kliesch S, Behre HM, Hertle L, Bergmann M. Alteration of Sertoli cell differentiation in the presence of carcinoma in situ in human testes. *J Urol* 1998;**160**:1894–8 PMID: 9783981.

[27] de Jong J, Stoop H, Gillis AJ, van Gurp RJ, van de Geijn GJ, Boer M, Hersmus R, Saunders PT, Anderson RA, Oosterhuis JW, Looijenga LH. Differential expression of SOX17 and SOX2 in germ cells and stem cells has biological and clinical implications. *J Pathol* 2008;**215**:21–30. doi:10.1002/path.2332.

[28] Skakkebaek NE, Rajpert-De Meyts E, Main KM. Testicular dysgenesis syndrome: an increasingly common developmental disorder with environmental aspects. *Hum Reprod* 2001;**16**:972–8. doi:10.1093/humrep/16.5.972.

[29] Rajpert-De Meyts E. Developmental model for the pathogenesis of testicular carcinoma in situ: genetic and environmental aspects. *Hum Reprod Update* 2006;**12**:303–23. doi:10.1093/humupd/dmk006.

[30] Looijenga LH, Gillis AJ, Stoop H, Biermann K, Oosterhuis JW. Dissecting the molecular pathways of (testicular) germ cell tumour pathogenesis; from initiation to treatment-resistance. *Int J Androl* 2011;**34**:e234–51. doi:10.1111/j.1365-2605.2011.01157.x.

[31] Zhang XS, Zhang ZH, Jin X, Wei P, Hu XQ, Chen M, Lu CL, Lue YH, Hu ZY, Sinha Hikim AP, et al. Dedifferentiation of adult monkey Sertoli cells through activation of extracellularly regulated kinase 1/2 induced by heat treatment. *Endocrinology* 2006;**147**:1237–45. doi:10.1210/en.2005-0981.

[32] Oosterhuis JW, Looijenga LH. Testicular germ-cell tumours in a broader perspective. *Nat Rev Cancer* 2005;**5**(3):210–22.

[33] Sharpe RM, Skakkebaek NE. Testicular dysgenesis syndrome: mechanistic insights and potential new downstream effects. *Fertil Steril* 2008;**89**:e33–8. doi:10.1016/j.fertnstert.2007.12.026.

[34] Amini P, Nassiri S, Malbon A, Markkanen E. Differential stromal reprogramming in benign and malignant naturally occurring canine mammary tumours identifies disease-modulating stromal components. *Sci Rep* 2020;**10**:5506. doi:10.1038/s41598-020-62354-8.

[35] Schumacher V, Gueler B, Looijenga LH, Becker JU, Amann K, Engers R, Dotsch J, Stoop H, Schulz W, Royer-Pokora B. Characteristics of testicular dysgenesis syndrome and decreased expression of SRY and SOX9 in Frasier syndrome. *Mol Reprod Dev* 2008;**75**:1484–94. doi:10.1002/mrd.20889.

[36] Eckert D, Nettersheim D, Heukamp LC, Kitazawa S, Biermann K, Schorle H. TCam-2 but not JKT-cells resemble seminoma in cell culture. *Cell Tissue Res* 2008;**331**:529–38. doi:10.1007/s00441-007-0527-y.

[37] de Jong J, Stoop H, Gillis AJ, Hersmus R, van Gurp RJ, van de Geijn GJ, van Drunen E, Beverloo HB, Schneider DT, Sherlock JK, et al. Further characterization of the first seminoma cell line TCam-2. *Genes Chromosomes Cancer* 2008;**47**:185–96. doi:10.1002/gcc.20520.

[38] Aumüller G, Peter S. Immunohistochemical and ultrastructural study of Sertoli cells in androgen insensitivity. *Int J Androl* 1986;**9**:108–99. doi:10.1111/j.1365-2605.1986.tb00872.x.

[39] Guminska A, Oszukowska E, Kuzanski W, Sosnowski M, Wolski JK, Walczak-Jedrzejowska R, Marchlewska K, Niedzielski J, Kula K, Slowikowska-Hilczer J. Less advanced testicular dysgenesis is associated by a higher prevalence of germ cell neoplasia. *Int J Androl* 2010;**33**:e153–62. doi:10.1111/j.1365-2605.2009.00981.x.

[40] Ku NO, Omary MB. Keratins turn over by ubiquitination in a phosphorylation-modulated fashion. *J Cell Biol* 2000;**149**:547–52. doi:10.1111/andr.301.

[41] Nettersheim D, Jostes S, Sharma R, Schneider S, Hofmann A, Ferreira HJ, Hoffmann P, Kristiansen G, Esteller MB, Schorle H. BMP Inhibition in Seminomas Initiates Acquisition of Pluripotency via NODAL Signaling Resulting in Reprogramming to an Embryonal Carcinoma. *PLoS Genet* 2015;**11**:e1005415. doi:10.1371/journal.pgen.1005415.

[42] Tarulli GA, Stanton PG, Loveland KL, Rajpert-De Meyts E, McLachlan RI, Meachem SJ. A survey of Sertoli cell differentiation in men after gonadotropin suppression and in testicular cancer. *Spermatogenesis* 2013;**3**:e24014. doi:10.4161/spmg.24014.

[43] Brehm R, Rüttinger C, Fischer P, Gashaw I, Winterhager E, Kliesch S, Bohle RM, Steger K, Bergmann M. Transition from preinvasive carcinoma in situ to seminoma is accompanied by a reduction of connexin 43 expression in Sertoli cells and germ cells. *Neoplasia* 2006;**8**(6):499–509. doi:10.1593/neo.05847.

[44] Nistal M, Pastrián LG, González-Peramato P, Miguel MP. Inhibin bodies: a new marker for immature Sertoli cells. *Histopathology* 2011;**58**:1019–27. doi:10.1111/j.1365-2559.2011.03858.x.

[45] Brehm R, Marks A, Rey R, Kliesch S, Bergmann M, Steger K. Altered expression of connexins 26 and 43 in Sertoli cells in seminiferous tubules infiltrated with carcinoma-in-situ or seminoma. *J Pathol* 2002;**197**:647–53. doi:10.1002/path.1140.

[46] Steger K, Rey R, Kliesch S, Louis F, Schleicher G, Bergmann M. Immunohistochemical detection of immature Sertoli cell markers in testicular tissue of infertile adult men: a preliminary study. *Int J Androl* 1996;**19**:122–8. doi:10.1111/j.1365-2605.1996.tb00448.x.

[47] Skakkebaek NE. Possible carcinoma-in-situ of the testis. *Lancet* 1972;**2**:516–17. doi:10.1016/s0140-6736(72)91909-5.

[48] Nielsen, H.; Nielsen, M.; Skakkebaek, N.E. The fine structure of a possible carcinoma-in-situ in the seminiferous tubules in the testis of four infertile men. *Acta path microbiol scand*, 1974, 82, 235-248. DOI: 10.1111/j.1699-0463.1974.tb03848.x

[49] Nistal M, Jimenez F, Paniagua R. Sertoli cell types in the Sertoli-cell-only syndrome: relationships between Sertoli cell morphology and aetiology. *Histopathology* 1990;**16**:173–80. doi:10.1111/j.1365-2559.1990.tb01086.x.

[50] Paniagua R, Nistal M, Bravo MP. The formation of annulate lamellae in the human Sertoli cell. *Archives of Andrology* 1984;**13**:9–14. doi:10.3109/01485018408987496.

[51] Fink C, Weigel R, Hembes T, Lauke-Wettwer H, Kliesch S, Bergmann M, Brehm RH. Altered expression of ZO-1 and ZO-2 in Sertoli cells and loss of blood-testis barrier integrity in testicular carcinoma in situ. *Neoplasia* 2006;**8**:1019–27. doi:10.1593/neo.06559.

[52] Fink C, Weigel R, Fink L, Wilhelm J, Kliesch S, Zeiler M, Bergmann M, Brehm R. Claudin-11 is over-expressed and dislocated from the blood-testis barrier in Sertoli cells associated with testicular intraepithelial neoplasia in men. *Histochem Cell Biol* 2009;**131**:755–64. doi:10.1007/s00418-009-0576-2.

[53] Hersmus R, de Leeuw BH, Wolffenbuttel KP, Drop SL, Oosterhuis JW, Cools M, Looijenga LHJ. New insights into type II germ cell tumor pathogenesis based on studies of patients with various forms of disorders of sex development (DSD). *Mol CellEndocrinol* 2008;**291**:1–10. doi:10.1016/j.mce.2008.02.028.

[54] Li Y, Vilain E, Conte F, Rajpert-De Meyts E, Lau YF. Testis-specific protein Y-encoded gene is expressed in early and late stages of gonadoblastoma and testicular carcinoma in situ. *Urol Oncol* 2007;**25**:141–6. doi:10.1016/j.urolonc.2006.08.002.

[55] Kao CS, Ulbright TM, Idrees MT. Gonadoblastoma: An immunohistochemical study and comparison to Sertoli cell nodule with intratubular germ cell neoplasia, with pathogenetic implications. *Histopathology* 2014;**65**:861–7. doi:10.1111/his.12444.